Regulation of flagellar motor switching by c-di-GMP phosphodiesterases in *Pseudomonas aeruginosa*

Received for publication, April 22, 2019, and in revised form, July 23, 2019 Published, Papers in Press, July 26, 2019, DOI 10.1074/jbc.RA119.009009

Lingyi Xin[‡1], Yukai Zeng[§1], Shuo Sheng[¶], Rachel Andrea Chea[‡], Qiong Liu[¶], Hoi Yeung Li[‡], Liang Yang[‡‖], Linghui Xu[¶‡‡], Keng-Hwee Chiam[§2], and Zhao-Xun Liang[‡**3]**

*From the [‡]School of Biological Sciences, the [‖]Interdisciplinary Graduate School, and the **Singapore Centre for Environmental Life Sciences Engineering, Nanyang Technological University, 637551, Singapore, the [§]Bioinformatics Institute (A*STAR), S138671, Singapore, and the [¶]Guangdong Innovative and Entrepreneurial Research Team of Sociomicrobiology Basic Science and Frontier Technology, Integrative Microbiology Research Centre and the [‡‡]Key Laboratory of Bio-Pesticide Innovation and Application of Guangdong Province, South China Agricultural University, Guangzhou 510642, China*

Edited by Roger J. Colbran

The second messenger cyclic diguanylate (c-di-GMP) plays a prominent role in regulating flagellum-dependent motility in the single-flagellated pathogenic bacterium *Pseudomonas aeruginosa*. The c-di-GMP–mediated signaling pathways and mechanisms that control flagellar output remain to be fully unveiled. Studying surface-tethered and free-swimming *P. aeruginosa* PAO1 cells, we found that the overexpression of an exogenous diguanylate cyclase (DGC) raises the global cellular c-di-GMP concentration and thereby inhibits flagellar motor switching and decreases motor speed, reducing swimming speed and reversal frequency, respectively. We noted that the inhibiting effect of c-di-GMP on flagellar motor switching, but not motor speed, is exerted through the c-di-GMP–binding adaptor protein MapZ and associated chemotactic pathways. Among the 22 putative c-di-GMP phosphodiesterases, we found that three of them (DipA, NbdA, and RbdA) can significantly inhibit flagellar motor switching and swimming directional reversal in a MapZ-dependent manner. These results disclose a network of c-di-GMP–signaling proteins that regulate chemotactic responses and flagellar motor switching in *P. aeruginosa* and establish MapZ as a key signaling hub that integrates inputs from different c-di-GMP–signaling pathways to control flagellar output and bacterial motility. We rationalized these experimental findings by invoking a model that postulates the regulation of flagellar motor switching by subcellular c-di-GMP pools.

Pseudomonas aeruginosa, a potentially lethal pathogenic bacterium for immune-compromised patients, relies on a single polar flagellum to swim in liquid and swarm across solid surfaces. Flagellum-dependent motility is essential for *P. aeruginosa* in establishing acute and chronic bacterial infections and evading host immune systems. Flagellum-dependent swimming motility enables the rapid dissemination of *P. aeruginosa* from the initial infection site of burn patients to cause potentially life-threatening systemic infections (1). The swimming motility also enables *P. aeruginosa* cells to navigate through mucus and interact with epithelial membranes to establish respiratory tract infection (2, 3). Flagellum-dependent motility is also crucial for establishing *P. aeruginosa* biofilm microcolonies (4–6), a hallmark of *P. aeruginosa*–dominated chronic infection (7). *P. aeruginosa* strains isolated from the airway of cystic fibrosis patients often lack the flagellum (8), and the loss of flagellum activities may be crucial for *P. aeruginosa* to evade assimilation and ingestion by phagocytes (9, 10). Hence, flagellum-dependent motility is considered a key pathogen-associated molecular pattern recognized by phagocytes to initiate engulfment.

Given the importance of flagellum-dependent motility in bacterial pathogenesis and host–pathogen interaction, *P. aeruginosa* has evolved sophisticated regulatory systems to control flagellar output. In recent years, the second messenger c-di-GMP[4] has emerged as a prominent regulator of flagellum-dependent motility. Existing data suggest that *P. aeruginosa* has evolved multiple c-di-GMP–dependent signaling pathways to regulate flagellum biosynthesis and motor output. Several c-di-GMP–metabolizing diguanylate cyclases (DGCs) and phosphodiesterases (PDEs) have been shown to impact flagellum-dependent motility in *P. aeruginosa* (11–14). Furthermore, a few c-di-GMP–binding effectors that mediate flagellar function at transcriptional or post-translational level were identified. At the transcriptional level, the c-di-GMP–binding transcriptional regulator FleQ regulates the biosynthesis of flagellar motor complex (15–17). At the post-translational level, the c-di-GMP–binding FlgZ interacts with the stator protein MotC to suppress swarming motility (18), and the c-di-GMP–

This work was supported by ARC Tier II Grant MOE2015-T2-2-026 (to Z.-X. L.) from the Ministry of Education of Singapore. The research is also supported by National Basic Research Program of China Program 973 Grant number 2015CB150600 (to L. X.) and Guangdong technological innovation strategy of special funds key areas of research and development program Grant 2018B020205003. The authors declare that they have no conflicts of interest with the contents of this article.

This article contains Tables S1 and S2 and Figs. S1 and S2.

[1] These authors contributed equally to this work.

[2] To whom correspondence may be addressed: Bioinformatics Institute (A*STAR), 30 Biopolis St., #07-01, S138671, Singapore.

[3] To whom correspondence may be addressed: School of Biological Sciences, Nanyang Technological University, 60 Nanyang Dr., S637551, Singapore. Tel.: 65-63167866; Fax: 65-67913856; E-mail: zxliang@ntu.edu.sg.

[4] The abbreviations used are: c-di-GMP, cyclic diguanylate; PDE, phosphodiesterase; DGC, diguanylate cyclase; MCP, methyl-accepting chemotaxis protein; CW, clockwise; CCW, counter-clockwise; Tn, transposon; ANOVA, analysis of variance; LSD, least squared difference.

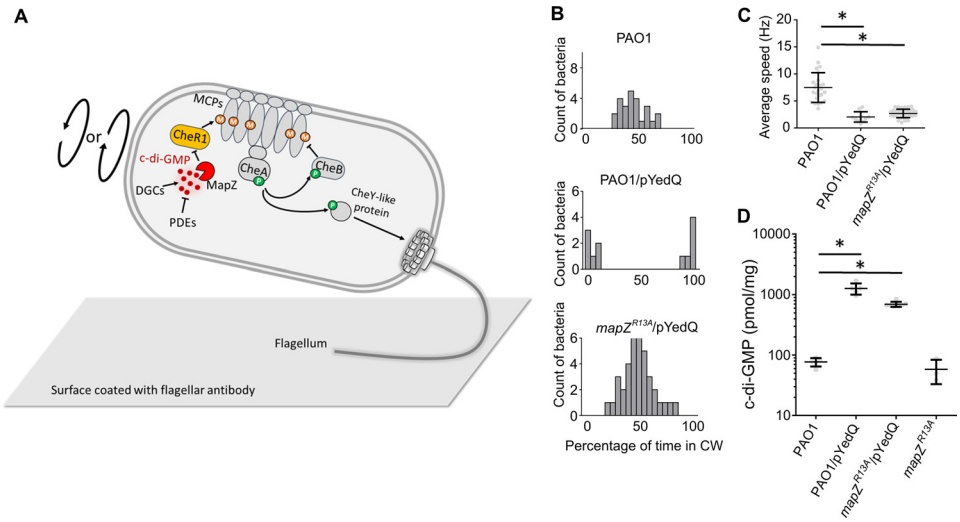

Figure 1. Expression of the exogenous diguanylate cyclase YedQ in *P. aeruginosa* PAO1 suppresses flagellar motor switching and motor speed. *A*, illustration of MapZ-mediated and c-di-GMP–dependent chemotaxis pathways and the bacterial cell-tethering assay. The MCPs from the chemoreceptor array detect chemoattractants and repellents and transduce the chemical signals to the autokinase CheA via the scaffolding protein CheW. A decrease in attractant binding activates the autokinase activity of CheA, and an increase in repellent binding suppresses the autokinase activity. When activated, CheA undergoes autophosphorylation and transfers the phosphoryl group to CheY, and the phosphorylated CheY binds to the flagellar switching complex to control flagellar rotation. The ligand-binding activity of MCPs is modulated by CheR and CheB, with CheR methylating specific glutamyl residues in MCPs and CheB removing the methyl groups. CheR and CheB constitutes an adaptation mechanism that constantly resets the MCPs to a prestimulus state as the bacterium travels through a ligand gradient (55). The adapter protein MapZ putatively senses the c-di-GMP pools, which are governed by the DGC and PDE proteins, to control the methylation of MCPs and the autokinase activity of CheA. *B*, bar graphs showing the percentage of time the bacterial cells spent in clockwise rotation obtained from the cell-tethering assays. The data suggest that motor switching in PAO1/pYedQ cells are greatly suppressed, whereas motor switching in PAO1 and *mapZ*^{R13A}/pYedQ cells is not suppressed. *C*, average motor speed for the PAO1, PAO1/pYedQ, and *mapZ*^{R13A}/pYedQ cells. The mean ± S.D. (n = 12–37 cells) data were obtained from two independent experiments. There was a significant effect of YedQ expression on average motor speed (two-way ANOVA, YedQ expression $F_{1,103} = 109.29$, $p < 0.0001$; *, $p < 0.01$ with LSD post hoc analysis). There was no significant effect of *mapZ*^{R13A} mutation or interaction on average motor speed (two-way ANOVA, *mapZ*^{R13A} mutation $F_{1,103} = 0.89$, $p = 0.3477$; interaction $F_{1,103} = 0.12$, $p = 0.7297$; $p > 0.01$ with LSD post hoc analysis). *D*, relative global cellular c-di-GMP levels of PAO1, PAO1/pYedQ, and *mapZ*^{R13A}/pYedQ strains measured using the HPLC method. The data were obtained from two independent experiments. There were significant effect of YedQ expression, *mapZ*^{R13A} mutation, and interaction on the relative global cellular c-di-GMP level (two-way ANOVA, YedQ expression $F_{1,16} = 195.02$, $p < 0.0001$; *mapZ*^{R13A} mutation $F_{1,16} = 20.46$, $p < 0.001$; interaction $F_{1,16} = 17.96$, $p < 0.001$; *, $p < 0.01$ with LSD post hoc analysis).

binding adaptor protein MapZ interacts with the chemotaxis methyltransferase CheR1 to inhibit flagellar motor switching (19, 20).

Our recent studies revealed that the c-di-GMP–binding adaptor protein MapZ plays a crucial role in regulating flagellar motor switching in *P. aeruginosa* (19–21). At high c-di-GMP concentrations, MapZ binds to the methyltransferase CheR1 and inhibits its enzymatic activity to decrease the methylation of multiple methyl-accepting chemotaxis proteins (MCPs) (22). The MapZ-mediated mechanism is likely to be operational in other *Pseudomonas* species considering *mapZ* is one of the most conserved nonessential genes in the genus of *Pseudomonas* (23). Although it was inferred that high cellular c-di-GMP levels would inhibit flagellar motor switching, the effect of elevated cellular c-di-GMP levels on motor switching has not been demonstrated. In this report, we present data to support the view that elevated cellular c-di-GMP concentrations inhibit flagellar motor switching and swimming reversal in a MapZ-dependent manner. We further reveal that 3 of 22 putative c-di-GMP PDEs of *P. aeruginosa* PAO1 act upstream of MapZ to exert control on flagellar motor switching. The results advance our understanding of how c-di-GMP regulates flagellum-dependent motility and disclose the unexpected roles of the three PDEs, DipA, NbdA, and RbdA, in controlling flagellar motor switching and bacterial motility.

Results

Overexpression of the exogenous DGC protein YedQ inhibits flagellar motor switching and suppresses motor speed

To determine how elevated cellular c-di-GMP concentrations impact flagellar motor activity, we transformed *P. aeruginosa* PAO1 cells with an overexpression plasmid that harbors the gene encoding the highly active *Escherichia coli* DGC protein YedQ. Overexpression of YedQ has been shown to raise the global concentration of c-di-GMP in *P. aeruginosa* and other bacterial cells (24–27). Overexpression of an exogenous instead of an endogenous DGC is expected to raise the global c-di-GMP level without perturbing any specific endogenous signaling pathways. The cell-tethering assay allowed us to directly monitor the motor output of the bacterial cells tethered to a surface using the flagellum-specific antibody (20, 28) (Fig. 1*A*). From the cell-tethering assays, we found that the PAO1/pYedQ cells exhibited greatly suppressed motor switching, with the majority of the cells undergoing unidirectional clockwise (CW) or counter-clockwise (CCW) rotation (Fig. 1*B*). The severely biased motor switching is in sharp contrast to the frequent motor switching exhibited by the PAO1 cells (19, 20). We previously found that the c-di-GMP–binding protein MapZ interacts with the chemotaxis methyltransferase CheR1 to regulate flagellar motor switching (20). To find out whether the inhibiting effect of YedQ expression on flagellar motor switch-

ing is exerted through MapZ, we overexpressed YedQ in a *mapZ*^{R13A} mutant strain that harbors a single chromosomal mutation (R13A) in the *mapZ* gene. Because Arg^{13} is essential for c-di-GMP binding, the MapZ^{R13A} mutant protein is defective in c-di-GMP binding and incapable of inhibiting CheR1 (19, 20). Remarkably, most *mapZ*^{R13A}/pYedQ cells exhibited similar bidirectional flagellar motor as the PAO1 cells (Fig. 1*B*).

When the average motor speed of the motile cells was measured, we found that the PAO1/pYedQ cells also exhibited a 3.1-fold lower motor speed than the PAO1 cells (Fig. 1*C*). The differences in motor output between the PAO1 and PAO1/pYedQ strains suggest that an elevated global c-di-GMP concentration can suppress both motor speed and motor switching. In contrast, the *mapZ*^{R13A}/pYedQ cells exhibited suppressed motor rotational speed, but normal motor switching behavior like the PAO1 cells (Fig. 1*C*). These observations strongly suggest that the suppression of motor speed is independent of MapZ. By using the well-established HPLC method (29, 30), we confirmed that the cellular c-di-GMP concentration of the PAO1/pYedQ strain is much higher than that of PAO1 (16-fold increase) (Fig. 1*D*). We noticed that the global cellular c-di-GMP level of the *mapZ*^{R13A}/pYedQ strain seemed to be slightly lower than that of the PAO1/pYedQ strain, whereas introducing the R13A mutation into the *mapZ* gene in PAO1 did not cause a significant decrease in the c-di-GMP level (Fig. 1*D*).

Taken together, the results confirm that MapZ is indispensable for c-di-GMP to exert its effect on motor switching and further suggest that MapZ does not seem to be required for motor speed control. Because the suppression on motor speed does not require MapZ, the dampening effect of c-di-GMP on motor speed is most likely exerted through another c-di-GMP–binding effector in the YedQ-expressing cells.

Overexpression of YedQ decreased swimming speed and directional reversal frequency

The single-flagellated *P. aeruginosa* cells swim following a "run–reverse–turn" pattern, which is distinct from the "run–tumble–run" pattern observed for *E. coli* cells (31). *P. aeruginosa* cells move forward ("run") when the motor undergoes CCW rotation and backward ("reversal") when the flagellum undergoes CW rotation (28). Considering the effect of high cellular c-di-GMP concentration on motor switching and rotational speed, it is logical to expect that the rise of cellular c-di-GMP concentration would influence flagellum-dependent swimming motility. By examining the trajectory of swimming bacterial cells using an inverted microscope, we observed that the PAO1 cells exhibit the typical run–reverse–turn trajectories that features sharp turn or reversal to change direction (Fig. 2*A*). On the contrary, most PAO1/pYedQ cells exhibited no turn or reversal and only ran in a single direction. This swimming pattern is consistent with the unidirectional motor rotation of the cells observed in the cell-tethering assays. Meanwhile, the *mapZ*^{R13A}/pYedQ cells are similar to the PAO1 cells by exhibiting frequent reversal of swimming direction, which is consistent with the frequent motor switching observed for the *mapZ*^{R13A}/pYedQ cells (Fig. 2*A*).

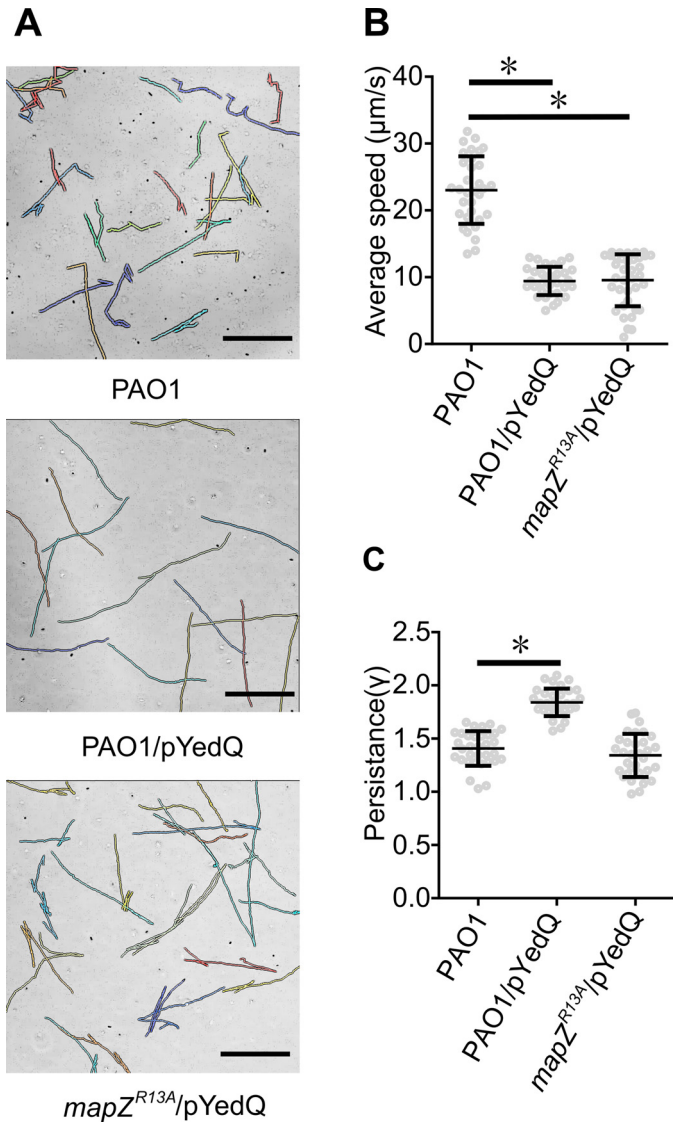

Figure 2. Expression of the exogenous diguanylate cyclase YedQ in *P. aeruginosa* PAO1 suppresses swimming reversal and decreases swimming speed. *A*, swimming trajectories show significantly less frequent directional reversal for the PAO1/pYedQ cells than the other two strains. *Scale bar*, 5 μm. *B*, average swimming speed of PAO1 and mutant cells to show that expression of YedQ decreases motor speed in a MapZ-independent manner. The data are means ± S.D. (n = 33–37 cells) from two independent experiments. There was a significant effect of YedQ expression on average swimming speed (two-way ANOVA, $F_{1,132}$ = 328.05, $p < 0.0001$; *, $p < 0.01$ with LSD post hoc analysis). There was no significant effect of *mapZ*^{R13A} mutation or interaction on average swimming speed (two-way ANOVA, *mapZ*^{R13A} mutation $F_{1,132}$ = 2.61, p = 0.1086; interaction $F_{1,132}$ = 3.13, p = 0.0792; $p >$ 0.01 with LSD post hoc analysis). *C*, swimming persistence of PAO1 and the mutant cells to show YedQ increases the persistence of runs in a MapZ-dependent manner. The calculation of the swimming persistence is described under "Materials and methods." The data are means ± S.D. (n = 32–33 cells) from two independent experiments. There were significant effects of YedQ expression, *mapZ*^{R13A} mutation, and interaction on swimming persistence (two-way ANOVA, YedQ expression $F_{1,127}$ = 9.34, $p < 0.01$; *mapZ*^{R13A} mutation $F_{1,127}$ = 27.22, $p < 0.0001$; interaction $F_{1,127}$ = 132.9, $p < 0.0001$; *, $p <$ 0.01 with LSD post hoc analysis).

From the swimming trajectories, we extracted the average swimming speed and persistence of runs, which is inversely proportional to the frequency of directional reversal. PAO1 cells exhibited 2.4-fold higher swimming speed than the other two mutant strains (Fig. 2*B*), in accordance with the different

motor speed observed for the three strains (Fig. 1*C*). The PAO1/pYedQ cells have a greater average persistence of runs than the PAO1 and *mapZ*^{R13A}/pYedQ cells (Fig. 2*C*), further supporting the role played by MapZ in inhibiting swimming reversal. The swimming behaviors of the three strains agree well with the motor speed and motor switching pattern observed in the cell-tethering assays. The results further support that elevated cellular c-di-GMP concentrations inhibit motor switching to decrease the frequency of swimming reversal via the MapZ-mediated mechanism.

Three endogenous c-di-GMP PDEs control flagellar motor switching

Having demonstrated that expression of an exogenous DGC can raise the global c-di-GMP level to inhibit motor switching, we next asked which endogenous DGCs or PDEs of *P. aeruginosa* are involved in the regulation of motor switching. Identifying the PDEs that control motor switching can be achieved by screening *pde* knockout mutants for inhibited motor switching, assuming the PDEs are constitutively expressed and active. However, identifying the DGCs that regulate motor switching is not so straightforward because we found that it is not possible to draw convincing conclusion from the *dgc* mutants because the effect of *dgc* deletion on flagellar switching seemed to be very subtle and rather difficult to reproduce among different batches of cultivated cells. Although the deletion of a *pde* gene can have a very strong phenotype because of the drastically suppressed motor switching as we show below, the deletion of a *dgc* gene does not alter the motor switching and swimming trajectory in a significant manner. For this reason, here we only focus on identifying the PDEs that regulate flagellar motor switching.

In *P. aeruginosa*, there are 22 proteins that are known or predicted to contain an enzymatically active EAL or HD-GYP–based PDE domain for degrading c-di-GMP (32–36). We performed cell-tethering assays for this comprehensive set of 22 *pde* transposon mutant strains to identify the ones that exhibit inhibited motor switching. We found that although a majority of *pde*::Tn mutants exhibited similar motor switching behavior as PAO1, with the cells capable of switching stochastically between the CW and CCW rotation modes (Fig. 3*A*), the three mutant strains *dipA*::Tn, *nbdA*::Tn, and *rbdA*::Tn exhibited drastically decreased frequency of motor switching as shown by the bimodal or trimodal pattern observed (Fig. 3, *A* and *B*). The *dipA*::Tn strain showed the greatest deviation from PAO1, with ~30% of the cells exhibiting unidirectional rotation and 70% exhibiting highly biased CW or CCW rotation. Also, unlike the PAO1 cells, the *rbdA*::Tn and *nbdA*::Tn cells exhibited highly biased CW or CCW rotation. Native promoter-driven expression of *dipA*, *nbdA*, and *rbdA* in the respective Tn mutant relieved the inhibition on motor switching (Fig. 3*C*), confirming that the suppression on motor switching is attributed to the absence of the PDEs. The three *pde* genes code for the multidomain proteins RbdA, NbdA, and DipA, respectively, with RbdA and NbdA containing a transmembrane domain (Fig. 3*D*). All three proteins were shown to contain an enzymatically active EAL domain and only function as c-di-GMP– degrading PDE without detectable DGC activity (37–39).

We also measured the motor speed of the motile cells for the 22 Tn mutant strains. None of the 22 transposon mutants exhibited significantly different motor speed relative to the PAO1 strains (Fig. S1). This is in contrast to the suppressing effect of YedQ expression on both motor switching and speed (Fig. 1*C*). Kulasekara *et al.* (40) recently reported that the deletion of the *dipA* orthologue *pch* in *P. aeruginosa* P14 also decreased swimming reversal, because of the inhibition of motor switching. It was also reported that the majority of the Δ*pch* cells were either nonmotile or swimming at a lower speed. We also observed that many *dipA*::Tn and *dipA*^{PDE*} cells were nonmotile, but those nonmotile cells were not included in our motor speed and velocity analysis.

The frequency of flagellar motor switching is correlated with the PDE activity of RbdA, NbdA, and DipA

To confirm that the inhibition of motor switching observed for the three transposon mutants is solely caused by the loss of PDE activity and thus an alteration of cellular c-di-GMP concentration, we introduced chromosomal mutation into the *dipA*, *nbdA*, or *rbdA* gene of PAO1 to replace the essential E(A/V)L motif in the EAL domain with an AAA motif to abolish the PDE activity (Fig. 4*A*) (32, 41). As expected, the resulted *rbdA*^{PDE*}, *nbdA*^{PDE*}, and *dipA*^{PDE*} mutant strains exhibited inhibited flagellar motor switching (Fig. 4*B*). The *rbdA*^{PDE*} and *nbdA*^{PDE*} strains showed even stronger motor switching bias than their corresponding transposon mutants with ~32% of the cells exhibiting unidirectional rotation. The results establish unambiguously that the inhibition of motor switching observed for the *pde* mutants is due to the loss of PDE activity and likely a rise of cellular c-di-GMP concentration.

To find out whether DipA, NbdA, and RbdA control flagellar motor switching through MapZ, we introduced the R13A mutation into the *mapZ* gene of the *rbdA*^{PDE*}, *nbdA*^{PDE*}, and *dipA*^{PDE*} strains to generate the three double mutant strains *rbdA*^{PDE*}&*mapZ*^{R13A}, *nbdA*^{PDE*}&*mapZ*^{R13A}, and *dipA*^{PDE*}&*mapZ*^{R13A}. The three double mutant strains harbor an enzymatically inactive PDE and a defective MapZ protein. The three double-mutant strains exhibited similar bidirectional flagellar motor switching pattern as the PAO1 strain (Fig. 4*B*), suggesting that motor switching is no longer inhibited when MapZ is defective. Based on the observations, we concluded that MapZ is essential for inhibiting flagellar motor switching, likely by acting as the binding effector that senses the c-di-GMP pool controlled by RbdA, NbdA, and DipA.

The ability of P. aeruginosa to reverse swimming direction depends on the PDE activity of DipA, NbdA, and RbdA

Given the strong inhibiting effect of PDE inactivation on motor switching, we further examined the swimming trajectories of the mutants to investigate whether swimming motility is affected by PDE inactivation. The swimming trajectories of *P. aeruginosa* PAO1 and the mutant cells were recorded following the same procedure described earlier. We found that the majority of the *rbdA*^{PDE*}, *nbdA*^{PDE*}, and *dipA*^{PDE*} cells have lost their ability to reverse swimming direction, as evidenced by the swimming trajectories that lack the sharp turns (Fig. 5*A*). This observation is in accordance with the highly suppressed

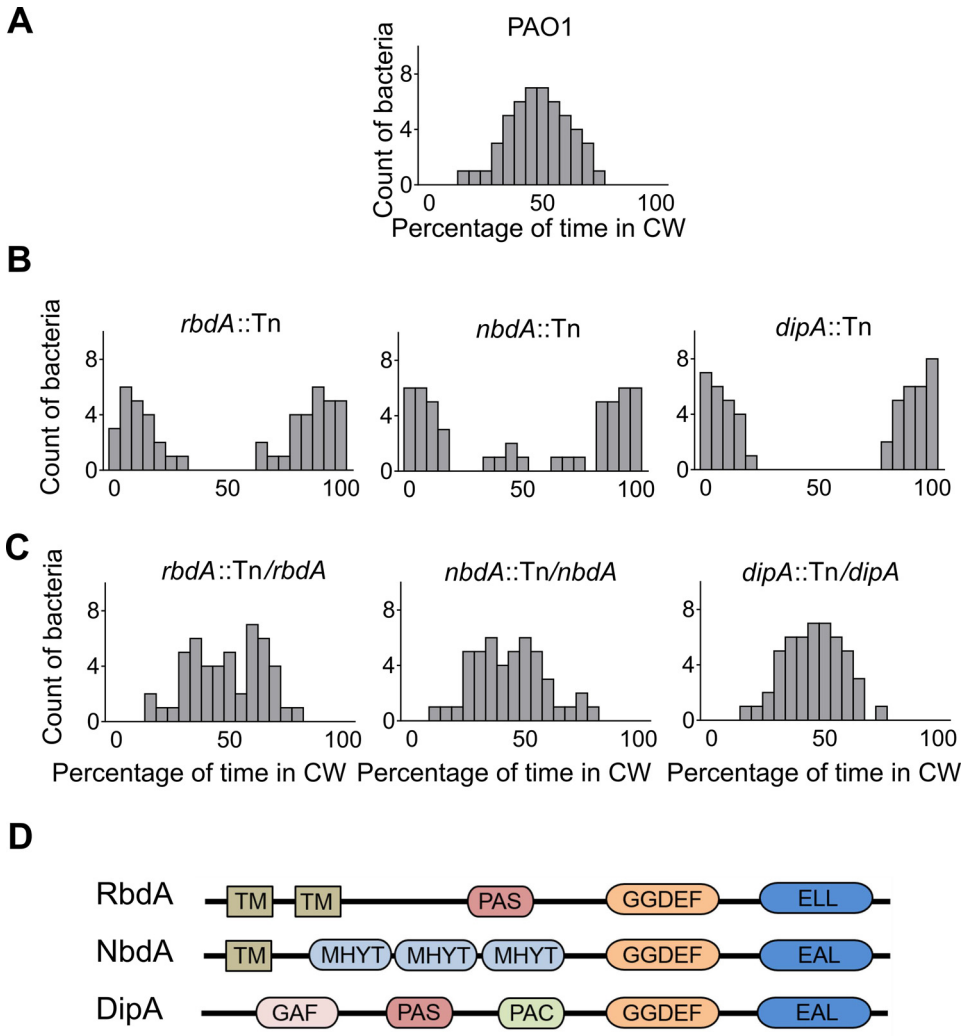

Figure 3. Identification of c-di-GMP PDEs that control flagellar motor switching by screening 22 transposon mutants. *A* and *B*, bar graphs generated from the data of cell-tethering assays showing the percentage of time spent in CW rotation for PAO1 and the three *pde*::*Tn* strains that showed severely repressed motor switching. *C*, bar graphs showing the percentage of time spent in CW rotation for the three complimentary mutants that exhibited a normal motor switching pattern. The data are means ± S.D. (n = 47–50 cells) from two independent experiments. *D*, domain organization of RbdA, NbdA, and DipA. *TM*, transmembrane motif. PAS/PAC, GAF, and MHYT are the putative sensory domains. The C-terminal EAL domains are the catalytically active PDE domains responsible for degrading c-di-GMP.

flagellar motor switching pattern for the three strains (Fig. 4*B*). In contrast, the double mutant strains *rbdA*^{PDE*}&*mapZ*^{R13A}, *nbdA*^{PDE*}&*mapZ*^{R13A}, and *dipA*^{PDE*}&*mapZ*^{R13A} exhibited the normal "run–turn–reversal" swimming trajectories with frequent directional reversal (Fig. 5*B*), reinforcing the crucial role of MapZ in controlling swimming directional reversal. As the result of inhibited motor switching, the *rbdA*^{PDE*}, *nbdA*^{PDE*}, and *dipA*^{PDE*} strains had greater persistence of runs than PAO1 and the double mutants (Fig. 5*C*). Meanwhile, the average swimming speed for the motile *rbdA*^{PDE*}, *nbdA*^{PDE*}, and *dipA*^{PDE*} cells does not seem to differ significantly from that of the PAO1 cells (Fig. 5*D*).

Impact of PDE inactivation on cellular c-di-GMP concentration

To probe whether there is a correlation between the inhibition of flagellar motor switching and a change in cellular c-di-GMP concentration, we measured the cellular c-di-GMP level of the 22 *pde*::Tn mutant strains using the P_{cdrA} promoter-fused green fluorescent protein (GFP) biosensor (42–44). We found that most mutant strains did not exhibit significantly altered c-di-GMP level than PAO1, and that the *dipA*::Tn and *rbdA*::Tn strains are the only two exhibiting noticeably higher c-di-GMP concentration (Fig. S2). Note that the 1.3- to 1.7-fold increase in c-di-GMP level for *dipA*::Tn and *rbdA*::Tn is much lower than the 16-fold increase observed for the PAO1/pYedQ strain. Also notable is that the *nbdA*::Tn mutant has a cellular c-di-GMP concentration comparable with that of PAO1 despite its suppressed motor switching phenotype. Measurement of the c-di-GMP concentration of the *rbdA*^{PDE*}, *nbdA*^{PDE*}, and *dipA*^{PDE*} strains confirmed that the inactivation of DipA and RbdA, but not NbdA, raised the cellular c-di-GMP level (Fig. S2). Consistent with our findings, it has been reported by others that *dipA* deletion led to an increase in cellular c-di-GMP concentration (37) and that the deletion of *nbdA* does not significantly affect the cellular c-di-GMP concentration (38). The unchanged c-di-GMP level in *nbdA*^{PDE*} cells suggests that effective inhibition of motor switching does not require a rise of global c-di-GMP level.

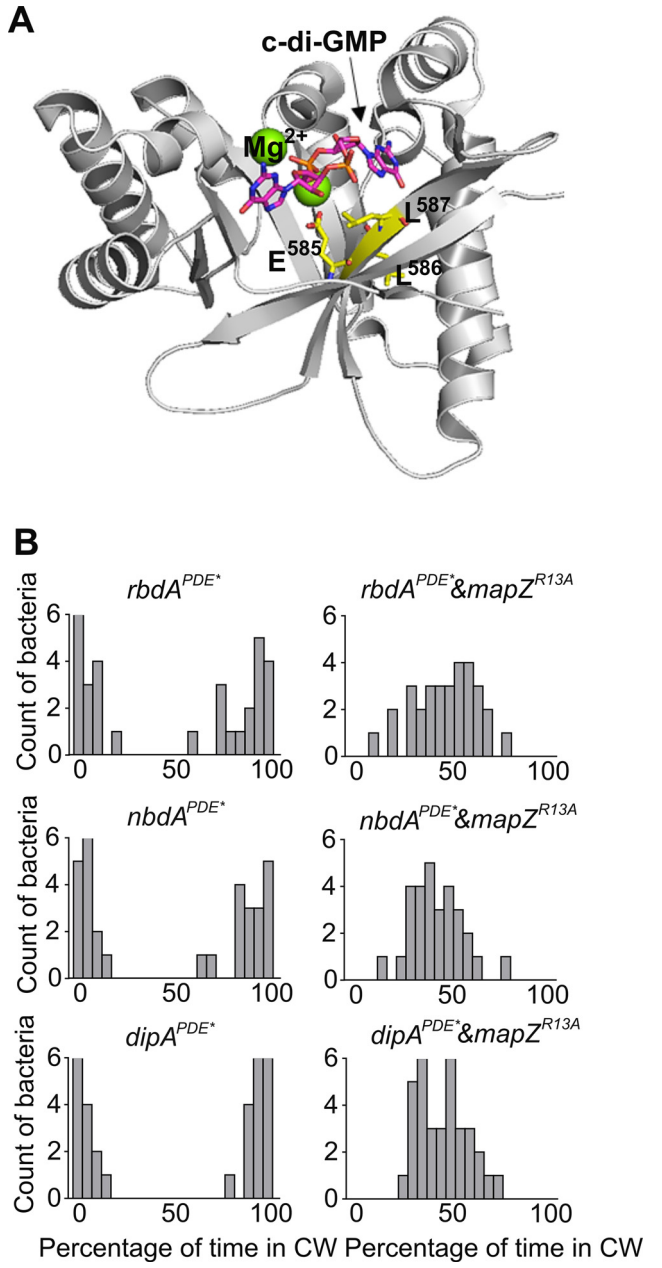

Figure 4. Inactivation of the PDE domain of RbdA, NbdA, and DipA inhibits flagellar motor switching in a MapZ-dependent manner. *A*, crystal structure of the EAL domain of RbdA showing the position and crucial role of the ELL motif in binding the metal ions and c-di-GMP (56). *B*, bar graphs showing the percentage of time spent in CW rotation for the three PDE inactive mutants and the three double mutants that harbor inactive PDE and defective MapZ. The data suggest that MapZ is indispensable for the inhibition of motor switching. The data are means ± S.D. (n = 29 to 34 cells) from two independent experiments.

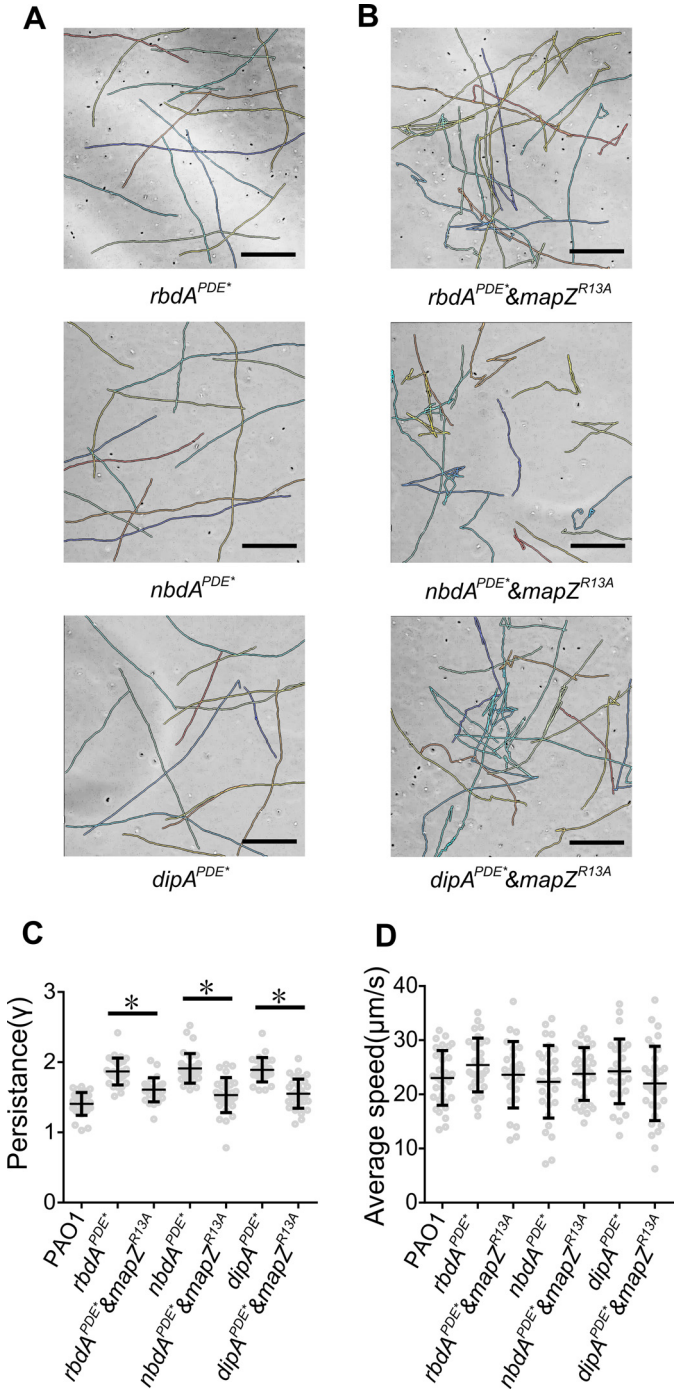

Figure 5. Inactivation of the PDE domain of RbdA, NbdA, and DipA suppresses directional reversal in swimming in a MapZ-dependent manner. *A*, swimming trajectories for the three PDE inactive mutants. *Scale bar*, 5 μm. *B*, swimming trajectories for the three double mutants that harbor a catalytically inactive PDE and a defective MapZ. *Scale bar*, 5 μm. The data suggest that MapZ is indispensable for the suppression of swimming reversal. *C*, comparison of directional swimming persistence. The calculation of the swimming persistence is described under "Materials and methods." The data are presented as means ± S.D. (n = 26–34 cells) from two independent experiments. There were significant effects of YedQ expression, $mapZ^{R13A}$ mutation, and interaction on swimming persistence (two-way ANOVA, YedQ expression $F_{3,238}$ = 20.45, $p < 0.0001$; $mapZ^{R13A}$ mutation $F_{1,238}$ = 62.41, $p < 0.0001$; interaction $F_{3,238}$ = 27.34, $p < 0.0001$; *, $p < 0.01$ with LSD post hoc analysis). *D*, comparison of average swimming speed. The data are presented as means ± S.D. (n = 26–34 cells) from two independent experiments.

Discussion

Adaptive control of flagellar motor output is vital for the success of *P. aeruginosa* as a versatile environmental bacterium and opportunistic pathogen. Although the role played by c-di-GMP in regulating flagellum-dependent motility is widely recognized (4, 5, 14, 45), the underlying molecular mechanisms remain to be fully understood. We performed the single-cell–based assays to demonstrate unequivocally that elevated global cellular c-di-GMP concentration can have profound impact on

flagellar motor speed and motor switching. The results are broadly consistent with the view that cellular c-di-GMP concentration is inversely correlated with bacterial motility (46, 47). In *P. aeruginosa*, c-di-GMP was already known to regulate motor speed and swarming motility via FlgZ, another c-di-GMP–binding PilZ adaptor (18). FlgZ dampens motor speed by interacting with the stator protein MotC at high c-di-GMP concentrations (18). In light of our recent and current findings that c-di-GMP can inhibit flagellar motor switching via the distinct MapZ-mediated mechanism (19, 20, 22), it is now evident that c-di-GMP can exert its control on flagellar output at the post-translational level via discrete mechanisms that involve FlgZ, MapZ, and potentially other yet-to-be identified c-di-GMP binding effectors.

Flagellar motor switching is known to be controlled by the chemosensory system, with rotational bias generated when a gradient of chemoattractant or chemorepellent is detected by the sensory domain of the MCPs. Just like the MCPs that contain sensory domains for detecting a diversity of chemoattractant and chemorepellents (48), DipA, NbdA, and RbdA also have sensory domains that putatively modulate the PDE activity. The environmental or cellular signals sensed by DipA, NbdA, and RbdA are likely to affect flagellar motor switching as well. Hence, the flagellar motor switching is subjected to the control of multiple signals that are integrated through the c-di-GMP and chemotactic signaling proteins. The complex signaling network with multiple inputting points presumably allows the bacteria to fine-tune their chemotactic responses and motility.

Our results suggest that the three c-di-GMP specific PDEs, DipA, NbdA, and RbdA, act through MapZ to control flagellar motor switching. Critically, the observation that inactivation of a single PDE (*i.e.* DipA, RbdA, or RbdA) resulted in the inhibition of motor switching cannot be rationalized by suggesting that the three PDEs contribute to a common global c-di-GMP pool. This is because logically such a common global c-di-GMP cannot be maintained at high levels to inhibit motor switching with two of the three PDEs actively depleting the c-di-GMP pool. Instead, the data are best rationalized by a model that invokes local c-di-GMP signaling, which is plausible with MapZ and the three PDEs co-localized on the periphery of the chemoreceptor arrays and in proximity to different MCPs (Fig. 6). Because of their association with different sets of MCPs, DipA, RbdA, and NbdA have their own sphere of influence and can control separate c-di-GMP pools to modulate the methylation of different MCPs (Fig. 6). A lack of correlation between global cellular c-di-GMP levels and the phenotypes generated by inactivation of individual DGCs and PDEs is already considered as a common phenomenon (45, 52–54). The phenomenon was rationalized by invoking mechanisms that involve subcellular localization of DGC/PDEs and highly specific local c-di-GMP signaling (45, 52–54). Similarly, the model illustrated in Fig. 6 emphasizes local c-di-GMP signaling and is broadly in line with some of those local c-di-GMP signaling models.

There is already existing evidence supporting our model and the localization of MapZ and two of the three PDEs next to the chemoreceptor arrays. MapZ was shown to localize at the cell pole through the interaction with the methyltransferase CheR1

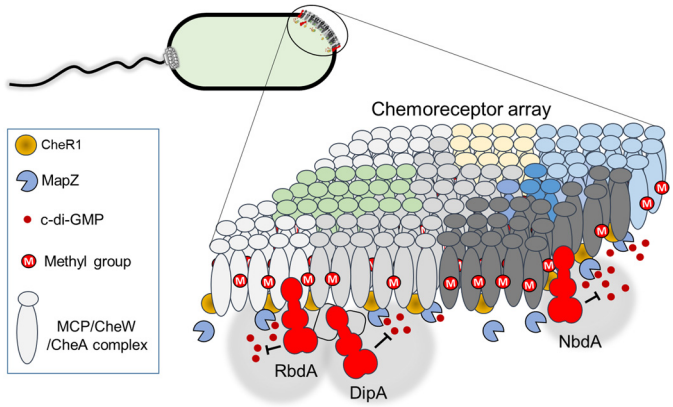

Figure 6. A model for the regulation of chemotaxis and flagellar motor switching by c-di-GMP and the three PDEs in *P. aeruginosa*. The model depicts the bacterial chemoreceptor arrays as highly organized sensory patches composed of thousands of transmembrane MCP proteins. DipA, RbdA, and NbdA are postulated to be situated in proximity to the MCPs-constituted chemoreceptor array and interacting with different MCPs. The *gray sphere* represents the sphere of influence of the three PDEs, which allow them to control separate c-di-GMP pools, and thus the methylation level of different sets of MCPs to control distinct chemotactic pathways.

(20). Pulldown experiments suggested that DipA and RbdA interact with the chemotactic proteins CheA and BdlA directly or indirectly (40, 49–51). Although the cellular localization of NbdA is unknown, the inner-membrane anchored NbdA, whose expression level was found to be low and tightly controlled (38), could also be positioned aside MCPs. Given their subcellular localization, we propose that DipA, RbdA, and NbdA act as drains to maintain separate local c-di-GMP pools near the chemoreceptor arrays to control the methylation of nearby MCPs. Through MapZ, the three PDEs control the auto-kinase activity of distinct sets of MCPs, and each set of the MCPs can perturb the dynamic equilibrium between CheY and phosphorylated CheY independently to impact motor switching.

In PAO1 cells, the 22 PDEs act as drains to maintain specific c-di-GMP pools together with their co-localized DGC partners. c-di-GMP pools can vary in size, which is decided by the diffusion distance of c-di-GMP before it is trapped and degraded by a PDE. c-di-GMP pools can also vary in depth, which represents the concentration range of the c-di-GMP pool. When a PDE is inactivated, the size and depth of its controlled c-di-GMP pool can increase significantly or only slightly, depending on the enzymatic activity of the PDE and its local DGC partners. Based on the observation that the cellular c-di-GMP level was not perturbed by the corresponding *pde*::Tn mutation, NbdA and most PDEs seem to only alter the size and depth of their local c-di-GMP pools moderately. Meanwhile, the observed increases in cellular c-di-GMP level for the *dipA* and *rbdA* mutants suggest that DipA and RbdA are highly active PDEs in degrading c-di-GMP and that the size and depth of the c-di-GMP pools governed by the two PDEs could undergo significant changes.

The realization that DipA and RbdA can significantly alter the size and depth of their c-di-GMP pools provides an explanation for the multiple phenotypes observed for the *dipA* and *rbdA* mutants (37–39, 56). DipA has been proposed to be one of the PDEs that enables *P. aeruginosa* to respond to the nutrient

levels in the environment, putatively by interacting with the chemotaxis system (57). In addition to its influence on motility, DipA also regulates the production of the Psl extracellular polysaccharide (37). RbdA is a positive regulator of bacterial motility and production of rhamnolipids and at the same time a negative regulator of extracellular polysaccharide production (39, 56). The observations that DipA and RbdA can regulate cellular functions unrelated to flagellar motor switching strongly suggest that the two PDEs can engage other downstream c-di-GMP–binding effectors than MapZ. We propose that the reason why DipA and RbdA can engage multiple c-di-GMP effectors is because the two PDEs can drastically alter the size and depth of the c-di-GMP pools by tuning their PDE activity. An increase in the c-di-GMP pool size allows c-di-GMP to reach the c-di-GMP effectors that are located further away, whereas a change in the depth enables the engagement of c-di-GMP effectors with a different c-di-GMP binding dynamic range than MapZ.

In summary, our work so far has unveiled a signaling network consisting of MapZ, the three PDEs, and potentially other yet-to-be identified proteins in regulating chemotaxis and flagellar motor switching. Some fundamental questions still remain to be answered about the intricacy of the signaling network. The identification of the key DGCs and c-di-GMP effectors in the next stage will yield further insights into this highly complex c-di-GMP signaling network.

Materials and methods

Bacterial strains and plasmids

The bacterial strains and plasmids used in this study are described in Table S1. The DNA fragments encoding full-length or truncated proteins were amplified by PCR from *P. aeruginosa* PAO1 genomic DNA and by using primers designed according to the published *P. aeruginosa* PAO1 genome sequence (58). The primers used for PCR and molecular cloning are summarized in Table S2. Some *P. aeruginosa* PAO1 mutant strains used in this study were obtained from the *P. aeruginosa* PAO1 transposon mutant library (59).

Preparation of the P. aeruginosa mutants

The *P. aeruginosa rbdA*, *nbdA*, and *dipA* mutants were prepared following a previously published protocol (20) using the allelic exchange vector pK18GT. Briefly, DNA fragments of 1,518 bp containing the *rbdA-E585A*&*L586A*&*L587A* gene, 1,593 bp containing the *nbdA-E551A*&*L553A* gene, and 1,455 bp containing the *dipA-E675A*&*L677A* gene construct were amplified from *P. aeruginosa* PAO1 genomic DNA by overlap extension PCR. The primers used are listed in Table S2, with primers 1 and 2 for upstream fragment amplification, primers 3 and 4 for downstream amplification, and primers 1 and 4 for full-length gene amplification. The PCR products were ligated into the vector pK18GT using Gibson Assembly® cloning kit (New England Biolabs) or T4 DNA ligase (New England Biolabs) to generate the suicide plasmids. The suicide plasmids were transformed into *E. coli* DH5α for the subsequent conjugation with PAO1 or $mapZ^{R13A}$ by triparental mating with the helper plasmid pRK600. The transconjugants were selected on *Pseudomonas* isolation agar plates (BD Biosciences) containing 60 μg/ml gentamycin. Positive colonies were selected on *Pseudomonas* isolation agar plates (BD Biosciences) containing 10% sucrose. Colonies that contain the correct mutation were identified by sequencing of the DNA fragment amplified using primers listed in Table S2.

Cell-tethering assay for the analysis of the flagellar rotation

The cell tethering assay was carried out as described before (20, 28). Single colonies were used to inoculate 10 ml of Luria–Bertani broth (BD Biosciences) that was kept shaking at 37 °C at 250 rpm for overnight. The culutures were diluted to $A_{600\ nm}$ of 0.2 using M9 medium and grown at 37 °C at 250 rpm until the cells reached the late-exponential growth phase at $A_{600\ nm}$ of 0.8. The cell cultures were then diluted 10-fold prior to the microfluidic experiments. The cell tethering assays were carried out by using a microfluidic stagnation flow device precoated with flagellar antibodies (60). Flagella were sheared off by passing the bacterial cells through a 34-gauge blunt end needle four times. The cells were loaded into the cell chamber of the flow device, and nontethered cells were washed away using M9 broth. The cells were visualized using an inverted microscope (Nikon TE2000U) under 40× objective. Videos of tethered bacteria were taken at 40 fps for 1–5 min using a CMOS camera (Thorlabs DCC1645). L-Serine (10 mM in M9 medium) (0.5% w/v) was used as the chemoattractant in the analysis of flagellar rotation in chemical gradient. The M9 solution blank and L-serine solution were rapidly and completely gated to expose the cells to a temporally precise chemoattractant signal. The gating of the chemoattractant was performed through flow deflection between the chemoattractant and buffer inlets (60). Flow deflection ensured that cells tethered in the stagnation flow chamber were shielded from the L-serine prior to the chemotaxis experiments. The rotation of the cells was monitored and recorded following the reported procedure (61). The time spent by each cell in the CW, CCW, or pause phases was tallied in 20-s intervals. Image processing of the tethered cells were carried out as previously described (62) with videos of the tethered cells converted to gray scale and the contrast of the cells adjusted (saturated pixels = 0.4, histogram stack) using ImageJ (National Institutes of Health, Bethesda, MD). Images of the cells were binarized to isolate them from the background for every frame in the video. The center of mass coordinates of the rotating cell bodies of each cell was measured from the obtained binarized image stack and imported into our in-house analysis program BTAP in MATLAB.

Swimming trajectory analysis

The swimming trajectories were observed as described before (20). Free swimming *P. aeruginosa* cells with their intact flagellum were grown to exponential phase ($A_{600\ nm}$ of 1.0) in LB medium, diluted to 1:500 in 0.9% NaCl containing 3% Ficoll (Sigma–Aldrich) before being loaded in cell chambers with a channel height of 20 μm, and observed in the middle of the chamber depth (away from the coverslip). The cells were visualized under 40× objective using an inverted microscope (Nikon TE2000U), and videos of bacteria were taken at 25 fps using a CMOS camera (Thorlabs DCC1645). Image with cell outlines were obtained using ImageJ (National Institutes of

Health), and bacterial swimming trajectories were obtained using particle segmentation and tracking algorithms as described previously (63, 64) and implemented through the Trackmate Plugin in Fiji (65). Briefly, the cell outlines in each image of the time-lapsed video were segmented and identified according to the difference of Gaussians approach (63). The segmented cell outlines were then tracked by linking the individual cell outlines from frame to frame using the linear assignment problem method (64). The average speed and directional persistence of individual swimming cells were then obtained from the trajectories from the time-lapsed videos.

The average speed of an individual swimming cell is calculated by averaging the distance moved by the cell between each frame divided by the time between frames. The directional persistence of an individual swimming cell is calculated as follows: the mean squared displacement of a tracked cell at any point in time with two-dimensional coordinates x and y, is denoted as r^2, where $r^2 = x^2 + y^2$. The movement of each cell is fitted with the relation $r^2 \alpha t^{\gamma}$, where t is the time that has passed since the start of the cell tracking, and γ is an exponent characterizing the persistence of cell swimming. When $\gamma = 1$, then $r^2 \alpha t$, and the displacement of the cell exhibits a random walk or diffusive behavior. When $\gamma = 2$, then $r^2 \alpha t^2$, and the displacement of the cell exhibits "ballistic" behavior where the cell swims with a constant speed. Thus, the exponent γ quantifies directional persistence, with a value closer to 1 denoting persistency and a value closer to 2 denoting randomness.

Measurement of cellular c-di-GMP level

The overall c-di-GMP concentrations in PAO1 and mutant strains were measured as described before with modification (29, 30, 66). Briefly, overnight cultures were diluted in LB medium and grown to $A_{600\,nm}$ of 1.0. culture (50 ml) were obtained and washed twice by ice-cold PBS. The cells were resuspended in 2.5 ml of ice-cold PBS and incubated at 100 °C for 5 min. Ice-cold 100% ethanol was added to a final concentration of 65%, and supernatant was removed after centrifugation. Extraction was repeated twice for each sample, and supernatant was dried and resuspended in 100 μl of water. 80 μl of each sample was analyzed by HPLC at 253 nm using a reverse-phase C_{18} Targa column (4.6 × 150 mm; 5 μm) and a flow rate of 1.0 ml/min in solvents (solvent A: 10 mM ammonium acetate in water; solvent B: 10 mM ammonium acetate in methanol). The following gradient was used to elute c-di-GMP within 10 min: 1% solvent B and 99% solvent A. For protein quantification, cultures (1 ml) were pelleted and resuspended in 1 ml of 0.1 M NaOH by heating for 15 min at 95 °C and subsequently performing standard Bradford assay (Bio-Rad). The measurements were repeated in triplicate, and final c-di-GMP levels were normalized to total cellular protein levels.

The overall c-di-GMP concentration in PAO1 and mutants strains were also measured using a GFP-based biosensor method for the 22 *pde*::Tn mutants and the three catalytically defective *dipA*, *nbdA*, and *rbdA* mutants (42–44). Briefly, the plasmid pCdrA::*gfp* encoding the fluorescence-based reporter for c-di-GMP was transformed into PAO1 and transposon mutant strains by electroporation. Overnight cultures were diluted to $A_{600\,nm}$ of 0.01 in LB medium and 200 μl of diluted cultures were transferred into 96-well plate. A TECAN Infinite 200 PRO plate reader was used to measure c-di-GMP concentration in planktonic cells based on *cdrA*::*gfp* fluorescence (excitation, 485 nm; emission, 530 nm; excitation bandwidth, 9 nm; and emission bandwidth, 20 nm; manual gain, 80), and growth was monitored by quantifying the absorbance at $A_{600\,nm}$. The measurements were recorded at 15-min intervals. The relative fluorescence of GFP at $A_{600\,nm}$ of 1.0 was used as a measure of c-di-GMP level per cell.

Statistical analysis

Two-way analysis of variance (ANOVA) was used for statistical analysis. Least squared difference (LSD) post hoc test was performed for multiple comparisons.

Author contributions—L. Xin, K.-H. C., and Z.-X. L. conceptualization; L. Xin, Y. Z., S. S., R. A. C., Q. L., K.-H. C., and Z.-X. L. data curation; L. Xin, Y. Z., S. S., R. A. C., Q. L., K.-H. C., and Z.-X. L. formal analysis; L. Xin, Y. Z., S. S., R. A. C., K.-H. C., and Z.-X. L. validation; L. Xin, Y. Z., S. S., R. A. C., Q. L., H. Y. L., L. Y., L. Xu, K.-H. C., and Z.-X. L. investigation; L. Xin, Y. Z., S. S., Q. L., H. Y. L., L.Y., L. Xu, K.-H. C., and Z.-X. L. methodology; L. Xin, Y. Z., K.-H. C., and Z.-X. L. writing-original draft; L. Xin, Y. Z., L. Xu, K.-H. C., and Z.-X. L. writing-review and editing; Y. Z., K.-H. C., and Z.-X. L. software; H. Y. L., L.Y., K.-H. C., and Z.-X. L. resources; L. Xu, K.-H. C., and Z.-X. L. supervision; L. Xu, K.-H. C., and Z.-X. L. funding acquisition; K.-H. C. and Z.-X. L. project administration.

References

1. Lyczak, J. B., Cannon, C. L., and Pier, G. B. (2000) Establishment of *Pseudomonas aeruginosa* infection: lessons from a versatile opportunist. *Microbes Infect.* **2,** 1051–1060 CrossRef Medline
2. Feldman, M., Bryan, R., Rajan, S., Scheffler, L., Brunnert, S., Tang, H., and Prince, A. (1998) Role of flagella in pathogenesis of *Pseudomonas aeruginosa* pulmonary infection. *Infect. Immun.* **66,** 43–51 Medline
3. Sadikot, R. T., Blackwell, T. S., Christman, J. W., and Prince, A. S. (2005) Pathogen-host interactions in *Pseudomonas aeruginosa* pneumonia. *Am. J. Resp. Crit. Care Med.* **171,** 1209–1223 CrossRef Medline
4. O'Toole, G. A., and Kolter, R. (1998) Flagellar and twitching motility are necessary for *Pseudomonas aeruginosa* biofilm development. *Mol. Microbiol* **30,** 295–304 CrossRef Medline
5. Caiazza, N. C., Merritt, J. H., Brothers, K. M., and O'Toole, G. A. (2007) Inverse regulation of biofilm formation and swarming motility by *Pseudomonas aeruginosa* PA14. *J. Bacteriol.* **189,** 3603–3612 CrossRef Medline
6. Klausen, M., Heydorn, A., Ragas, P., Lambertsen, L., Aaes-Jørgensen, A., Molin, S., and Tolker-Nielsen, T. (2003) Biofilm formation by *Pseudomonas aeruginosa* wild type, flagella and type IV pili mutants. *Mol. Microbiol.* **48,** 1511–1524 CrossRef Medline
7. Costerton, J. W. (2001) Cystic fibrosis pathogenesis and the role of biofilms in persistent infection. *Trends Microbiol.* **9,** 50–52 CrossRef Medline
8. Luzar, M. A., Thomassen, M. J., and Montie, T. C. (1985) Flagella and motility alterations in *Pseudomonas aeruginosa* strains from patients with cystic fibrosis: relationship to patient clinical condition. *Infect. Immun.* **50,** 577–582 Medline
9. Amiel, E., Lovewell, R. R., O'Toole, G. A., Hogan, D. A., and Berwin, B. (2010) *Pseudomonas aeruginosa* evasion of phagocytosis is mediated by loss of swimming motility and is independent of flagellum expression. *Infect. Immun.* **78,** 2937–2945 CrossRef Medline
10. Lovewell, R. R., Hayes, S. M., O'Toole, G. A., and Berwin, B. (2014) *Pseudomonas aeruginosa* flagellar motility activates the phagocyte PI3K/Akt pathway to induce phagocytic engulfment. *Am. J. Physiol. Lung Cell Mol. Physiol.* **306,** L698–L707 CrossRef Medline

11. Ha, D. G., Richman, M. E., and O'Toole, G. A. (2014) Deletion mutant library for investigation of functional outputs of cyclic diguanylate metabolism in *Pseudomonas aeruginosa* PA14. *Appl. Environ. Microbiol.* **80,** 3384–3393 CrossRef Medline
12. Merritt, J. H., Brothers, K. M., Kuchma, S. L., and O'Toole, G. A. (2007) SadC reciprocally influences biofilm formation and swarming motility via modulation of exopolysaccharide production and flagellar function. *J. Bacteriol.* **189,** 8154–8164 CrossRef Medline
13. Merritt, J. H., Ha, D. G., Cowles, K. N., Lu, W., Morales, D. K., Rabinowitz, J., Gitai, Z., and O'Toole, G. A. (2010) Specific control of *Pseudomonas aeruginosa* surface-associated behaviors by two c-di-GMP diguanylate cyclases. *mBio* **1,** e00183-00110 Medline
14. Kuchma, S. L., Brothers, K. M., Merritt, J. H., Liberati, N. T., Ausubel, F. M., and O'Toole, G. A. (2007) BifA, a cyclic-di-GMP phosphodiesterase, inversely regulates biofilm formation and swarming motility by *Pseudomonas aeruginosa* PA14. *J. Bacteriol* **189,** 8165–8178 CrossRef Medline
15. Baraquet, C., Murakami, K., Parsek, M. R., and Harwood, C. S. (2012) The FleQ protein from *Pseudomonas aeruginosa* functions as both a repressor and an activator to control gene expression from the pel operon promoter in response to c-di-GMP. *Nucleic Acids Res.* **40,** 7207–7218 CrossRef Medline
16. Matsuyama, B. Y., Krasteva, P. V., Baraquet, C., Harwood, C. S., Sondermann, H., Navarro, M. V. (2016) Mechanistic insights into c-di-GMP–dependent control of the biofilm regulator FleQ from *Pseudomonas aeruginosa*. *Proc. Natl. Acad. Sci. U.S.A.* **113,** E209–E218 CrossRef Medline
17. Hickman, J. W., and Harwood, C. S. (2008) Identification of FleQ from *Pseudomonas aeruginosa* as a c-di-GMP-responsive transcription factor. *Mol. Microbiol.* **69,** 376–389 CrossRef Medline
18. Baker, A. E., Diepold, A., Kuchma, S. L., Scott, J. E., Ha, D. G., Orazi, G., Armitage, J. P., and O'Toole, G. A. (2016) PilZ domain protein FlgZ mediates cyclic di-GMP-dependent swarming motility control in *Pseudomonas aeruginosa*. *J. Bacteriol* **198,** 1837–1846 CrossRef Medline
19. Yan, X.-F., Xin, L., Yen, J. T., Zeng, Y., Jin, S., Cheang, Q. W., Fong, R. A. C. Y., Chiam, K.-H., Liang, Z.-X., and Gao, Y.-G. (2018) Structural analyses unravel the molecular mechanism of cyclic di-GMP regulation of bacterial chemotaxis via a PilZ adaptor protein. *J. Biol. Chem.* **293,** 100–111 CrossRef Medline
20. Xu, L., Xin, L., Zeng, Y., Yam, J. K. H., Ding, Y., Venkataramani, P., Cheang, Q. W., Yang, X., Tang, X., Zhang, L.-H., Chiam, K.-H., Yang, L., and Liang, Z.-X. (2016) A cyclic di-GMP–binding adaptor protein interacts with a chemotaxis methyltransferase to control flagellar motor switching. *Sci. Signal.* **9,** ra102 CrossRef Medline
21. Cheang, Q. W., Xin, L., Chea, R. Y. F., and Liang, Z.-X. (2019) Emerging paradigms for PilZ domain–mediated c-di-GMP signaling. *Biochem. Soc. Trans.* **47,** 381–388 CrossRef Medline
22. Sheng, S., Xin, L., Yam, J. K. H., Salido, M. M., Khong, N. Z. J., Liu, Q., Chea, R. A., Li, H. Y., Yang, L., Liang, Z.-X., and Xu, L. (2019) The MapZ-mediated methylation of chemoreceptors contributes to pathogenicity of *Pseudomonas aeruginosa*. *Front. Microbiol.* **10,** 67 CrossRef Medline
23. Dötsch, A., Klawonn, F., Jarek, M., Scharfe, M., Blöcker, H., and Häussler, S. (2010) Evolutionary conservation of essential and highly expressed genes in *Pseudomonas aeruginosa*. *BMC Genomics* **11,** 234 CrossRef Medline
24. Sanchez-Torres, V., Hu, H., and Wood, T. K. (2011) GGDEF proteins YeaI, YedQ, and YfiN reduce early biofilm formation and swimming motility in *Escherichia coli*. *Appl. Microbiol. Biotechnol.* **90,** 651–658 CrossRef Medline
25. Wang, T., Cai, Z., Shao, X., Zhang, W., Xie, Y., Zhang, Y., Hua, C., Schuster, S. C., Yang, L., and Deng, X. (2019) The pleiotropic effects of c-di-GMP content in *Pseudomonas syringae*. *Appl. Environ. Microbiol.* **85,** e00152-19 Medline
26. Chen, Y., Yuan, M., Mohanty, A., Yam, J. K., Liu, Y., Chua, S. L., Nielsen, T. E., Tolker-Nielsen, T., Givskov, M., Cao, B., and Yang, L. (2015) Multiple diguanylate cyclase-coordinated regulation of pyoverdine synthesis in *Pseudomonas aeruginosa*. *Environ. Microbiol. Rep.* **7,** 498–507 CrossRef Medline
27. Gjermansen, M., Ragas, P., and Tolker-Nielsen, T. (2006) Proteins with GGDEF and EAL domains regulate *Pseudomonas putida* biofilm formation and dispersal. *FEMS Microbiol. Lett.* **265,** 215–224 CrossRef Medline
28. Qian, C., Wong, C. C., Swarup, S., and Chiam, K. H. (2013) Bacterial tethering analysis reveals a "run-reverse-turn" mechanism for *Pseudomonas* species motility. *Appl. Environ. Microbiol.* **79,** 4734–4743 CrossRef Medline
29. Petrova, O. E., and Sauer, K. (2017) High-performance liquid chromatography (HPLC)-based detection and quantitation of cellular c-di-GMP. *Methods Mol. Biol.* **1657,** 33–43 CrossRef Medline
30. Roy, A. B., Petrova, O. E., and Sauer, K. (2013) Extraction and quantification of cyclic di-GMP from *P. aeruginosa*. *Bio. Protoc.* **3,** e828 Medline
31. Wadhams, G. H., and Armitage, J. P. (2004) Making sense of it all: bacterial chemotaxis. *Nat. Rev. Mol. Cell Biol.* **5,** 1024–1037 CrossRef Medline
32. Rao, F., Yang, Y., Qi, Y., and Liang, Z. X. (2008) Catalytic mechanism of c-di-GMP specific phosphodiesterase: a study of the EAL domain-containing RocR from *Pseudomonas aeruginosa*. *J. Bacteriol.* **190,** 3622–3631 CrossRef Medline
33. Rao, F., Qi, Y., Chong, H. S., Kotaka, M., Li, J., Lescar, J., Tang, K., and Liang, Z.-X. (2009) The functional role of a conserved loop in EAL domain-based c-di-GMP specific phosphodiesterase. *J. Bacteriol.* **191,** 4722–4731 CrossRef Medline
34. Römling, U., Liang, Z. X., and Dow, J. M. (2017) Progress in understanding of the molecular basis underlying functional diversification of cyclic dinucleotide turnover proteins. *J. Bacteriol.* **199,** e00790-16 Medline
35. Kulasakara, H., Lee, V., Brencic, A., Liberati, N., Urbach, J., Miyata, S., Lee, D. G., Neely, A. N., Hyodo, M., Hayakawa, Y., Ausubel, F. M., and Lory, S. (2006) Analysis of *Pseudomonas aeruginosa* diguanylate cyclases and phosphodiesterases reveals a role for bis-(3′-5′)-cyclic-GMP in virulence. *Proc. Natl. Acad. Sci. U.S.A.* **103,** 2839–2844 CrossRef Medline
36. Bellini, D., Caly, D. L., McCarthy, Y., Bumann, M., An, S. Q., Dow, J. M., Ryan, R. P., and Walsh, M. A. (2014) Crystal structure of an HD-GYP domain cyclic-di-GMP phosphodiesterase reveals an enzyme with a novel trinuclear catalytic iron centre. *Mol. Microbiol.* **91,** 26–38 CrossRef Medline
37. Roy, A. B., Petrova, O. E., and Sauer, K. (2012) The phosphodiesterase DipA (PA5017) is essential for *Pseudomonas aeruginosa* biofilm dispersion. *J. Bacteriol.* **194,** 2904–2915 CrossRef Medline
38. Li, Y., Heine, S., Entian, M., Sauer, K., and Frankenberg-Dinkel, N. (2013) NO-induced biofilm dispersion in *Pseudomonas aeruginosa* is mediated by an MHYT domain-coupled phosphodiesterase. *J. Bacteriol.* **195,** 3531–3542 CrossRef Medline
39. An, S., Wu, J., Zhang, L.-H. (2010) Modulation of *Pseudomonas aeruginosa* biofilm dispersal by a cyclic-di-GMP phosphodiesterase with a putative hypoxia-sensing domain. *Appl. Environ. Microbiol.* **76,** 8160–8173 CrossRef Medline
40. Kulasekara, B. R., Kamischke, C., Kulasekara, H. D., Christen, M., Wiggins, P. A., and Miller, S. I. (2013) c-di-GMP heterogeneity is generated by the chemotaxis machinery to regulate flagellar motility. *Elife* **2,** e01402 CrossRef Medline
41. Chen, M. W., Kotaka, M., Vonrhein, C., Bricogne, G., Rao, F., Chuah, M. L., Svergun, D., Schneider, G., Liang, Z. X., and Lescar, J. (2012) Structural insights into the regulatory mechanism of the response regulator RocR from *Pseudomonas aeruginosa* in cyclic Di-GMP signaling. *J. Bacteriol.* **194,** 4837–4846 CrossRef Medline
42. Fong, J., Yuan, M., Jakobsen, T. H., Mortensen, K. T., Delos Santos, M. M., Chua, S. L., Yang, L., Tan, C. H., Nielsen, T. E., and Givskov, M. (2017) Disulfide bond-containing ajoene analogues as novel quorum sensing inhibitors of *Pseudomonas aeruginosa*. *J. Med. Chem.* **60,** 215–227 CrossRef Medline
43. Nair, H. A., Periasamy, S., Yang, L., Kjelleberg, S., and Rice, S. A. (2017) Real time, spatial, and temporal mapping of the distribution of c-di-GMP during biofilm development. *J. Biol. Chem.* **292,** 477–487 CrossRef Medline
44. Rybtke, M. T., Borlee, B. R., Murakami, K., Irie, Y., Hentzer, M., Nielsen, T. E., Givskov, M., Parsek, M. R., and Tolker-Nielsen, T. (2012) Fluorescence-based reporter for gauging cyclic di-GMP levels in *Pseudomonas aeruginosa*. *Appl. Environ. Microbiol.* **78,** 5060–5069 CrossRef Medline

45. Kuchma, S. L., Ballok, A. E., Merritt, J. H., Hammond, J. H., Lu, W., Rabinowitz, J. D., and O'Toole, G. A. (2010) Cyclic-di-GMP–mediated repression of swarming motility by *Pseudomonas aeruginosa*: the pilY1 gene and its impact on surface-associated behaviors. *J. Bacteriol.* **192,** 2950–2964 CrossRef Medline
46. McCarter, L. L., and Gomelsky, M. (2015) Fifty ways to inhibit motility via cyclic di-GMP: the emerging *Pseudomonas aeruginosa* swarming story. *J. Bacteriol.* **197,** 406–409 CrossRef Medline
47. Römling, U., Galperin, M. Y., and Gomelsky, M. (2013) Cyclic di-GMP: the first 25 years of a universal bacterial second messenger. *Microbiol Mol. Biol. Rev.* **77,** 1–52 CrossRef Medline
48. Ortega, D. R., Fleetwood, A. D., Krell, T., Harwood, C. S., Jensen, G. J., and Zhulin, I. B. (2017) Assigning chemoreceptors to chemosensory pathways in *Pseudomonas aeruginosa*. *Proc. Natl. Acad. Sci. U.S.A.* **114,** 12809–12814 CrossRef Medline
49. Morgan, R., Kohn, S., Hwang, S. H., Hassett, D. J., and Sauer, K. (2006) BdlA, a chemotaxis regulator essential for biofilm dispersion in *Pseudomonas aeruginosa*. *J. Bacteriol.* **188,** 7335–7343 CrossRef Medline
50. Petrova, O. E., and Sauer, K. (2012) Dispersion by *Pseudomonas aeruginosa* requires an unusual posttranslational modification of BdlA. *Proc. Natl. Acad. Sci. U.S.A.* **109,** 16690–16695 CrossRef Medline
51. Li, Y., Petrova, O. E., Su, S., Lau, G. W., Panmanee, W., Na, R., Hassett, D. J., Davies, D. G., and Sauer, K. (2014) BdlA, DipA and induced dispersion contribute to acute virulence and chronic persistence of *Pseudomonas aeruginosa*. *PLoS Pathog.* **10,** e1004168 CrossRef Medline
52. Sarenko, O., Klauck, G., Wilke, F. M., Pfiffer, V., Richter, A. M., Herbst, S., Kaever, V., and Hengge, R. (2017) More than enzymes that make or break cyclic di-GMP: local signaling in the interactome of GGDEF/EAL domain proteins of *Escherichia coli*. *mBio* **8,** e01639-01617 Medline
53. Massie, J. P., Reynolds, E. L., Koestler, B. J., Cong, J.-P., Agostoni, M., and Waters, C. M. (2012) Quantification of high-specificity cyclic diguanylate signaling. *Proc. Natl. Acad. Sci. U.S.A.* **109,** 12746–12751 CrossRef Medline
54. Jenal, U., Reinders, A., and Lori, C. (2017) Cyclic di-GMP: second messenger extraordinaire. *Nat. Rev. Microbiol.* **15,** 271–284 CrossRef Medline
55. Sampedro, I., Parales, R. E., Krell, T., and Hill, J. E. (2015) *Pseudomonas* chemotaxis. *FEMS Microbiol. Rev.* **39,** 17–46 Medline
56. Liu, C., Liew, C. W., Wong, Y. H., Tan, S. T., Poh, W. H., Manimekalai, M. S. S., Rajan, S., Xin, L., Liang, Z.-X., Grüber, G., Rice, S. A., and Lescar, J. (2018) Insights into biofilm dispersal regulation from the crystal structure of the PAS-GGDEF-EAL region of RbdA from *Pseudomonas aeruginosa*. *J Bacteriol* **200,** e00515-00517 Medline
57. Mattingly, A. E., Kamatkar, N. G., Morales-Soto, N., Borlee, B. R., and Shrout, J. D. (2018) Multiple environmental factors influence the importance of the phosphodiesterase DipA upon *Pseudomonas aeruginosa* swarming. *Appl Environ Microbiol* **84,** e02847-02817 Medline
58. Stover, C. K., Pham, X. Q., Erwin, A. L., Mizoguchi, S. D., Warrener, P., Hickey, M. J., Brinkman, F. S., Hufnagle, W. O., Kowalik, D. J., Lagrou, M., Garber, R. L., Goltry, L., Tolentino, E., Westbrock-Wadman, S., Yuan, Y., *et al.* (2000) Complete genome sequence of *Pseudomonas aeruginosa* PAO1, an opportunistic pathogen. *Nature* **406,** 959–964 CrossRef Medline
59. Jacobs, M. A., Alwood, A., Thaipisuttikul, I., Spencer, D., Haugen, E., Ernst, S., Will, O., Kaul, R., Raymond, C., Levy, R., Chun-Rong, L., Guenthner, D., Bovee, D., Olson, M. V., and Manoil, C. (2003) Comprehensive transposon mutant library of *Pseudomonas aeruginosa*. *Proc. Natl. Acad. Sci. U.S.A.* **100,** 14339–14344 CrossRef Medline
60. Alicia, T. G., Yang, C., Wang, Z., and Nguyen, N. T. (2016) Combinational concentration gradient confinement through stagnation flow. *Lab. Chip* **16,** 368–376 CrossRef Medline
61. Wang, C. J., Bergmann, A., Lin, B., Kim, K., and Levchenko, A. (2012) Diverse sensitivity thresholds in dynamic signaling responses by social amoebae. *Sci. Signal.* **5,** ra17 Medline
62. Long, Z., Olliver, A., Brambilla, E., Sclavi, B., Lagomarsino, M. C., and Dorfman, K. D. (2014) Measuring bacterial adaptation dynamics at the single-cell level using a microfluidic chemostat and time-lapse fluorescence microscopy. *Analyst* **139,** 5254–5262 CrossRef Medline
63. Lowe, D. G. Distinctive image features from scale-invariant keypoints. *Int. J. Comput. Vis.* **60,** 91–110
64. Jaqaman, K., Loerke, D., Mettlen, M., Kuwata, H., Grinstein, S., Schmid, S. L., and Danuser, G. (2008) Robust single-particle tracking in live-cell time-lapse sequences. *Nat. Methods* **5,** 695–702 CrossRef Medline
65. Schindelin, J., Arganda-Carreras, I., Frise, E., Kaynig, V., Longair, M., Pietzsch, T., Preibisch, S., Rueden, C., Saalfeld, S., Schmid, B., Tinevez, J.-Y., White, D. J., Hartenstein, V., Eliceiri, K., Tomancak, P., and Cardona, A. (2012) Fiji: an open-source platform for biological-image analysis. *Nat. Methods* **9,** 676–682 CrossRef Medline
66. Spangler, C., Böhm, A., Jenal, U., Seifert, R., and Kaever, V. (2010) A liquid chromatography-coupled tandem mass spectrometry method for quantitation of cyclic di-guanosine monophosphate. *J. Microbiol. Methods* **81,** 226–231 CrossRef Medline

Regulation of flagellar motor switching by c-di-GMP phosphodiesterases in *Pseudomonas aeruginosa*

Lingyi Xin, Yukai Zeng, Shuo Sheng, Rachel Andrea Chea, Qiong Liu, Hoi Yeung Li, Liang Yang, Linghui Xu, Keng-Hwee Chiam and Zhao-Xun Liang

J. Biol. Chem. 2019, 294:13789-13799.
doi: 10.1074/jbc.RA119.009009 originally published online July 26, 2019